Supporting Information

Simultaneous Removal of Multiple Heavy Metal Ions from River Water Using Ultra-Fine Mesoporous Magnetite Nanoparticles

Tano Patrice Fato,[†] Da-Wei Li,[†] Li-Jun Zhao,[†] Kaipei Qiu,[,†] and Yi-Tao Long[†,‡]*

† School of Chemistry and Molecular Engineering, East China University of Science and Technology, 130 Meilong Road, Shanghai 200237, China.

‡ State Key Laboratory of Analytical Chemistry for Life Science, School of Chemistry and Chemical Engineering, Nanjing University, 163 Xianlin Avenue, Nanjing 210039, China

*E-mail: qiukaipei@ecust.edu.cn; Tel/Fax 86-21-64252339

Contents

1. Experimental section……S3

1.1. Reagents and materials……...…S3

1.2. Synthesis procedure of Fe_3O_4 nanoparticles ……S4

1.3. Metal ions removal procedure ……..S4

1.4. Point of zero charge measurement ……...S6

2.Characterization of the UFMNPs ……..…...S6

2.1. Brunauer-Emmett-Teller study after adsorption ……....S6

2.2. Scanning electron microscope/energy-dispersive X-ray analysis ……...S7

3.Tests of the metal ions adsorption……....S9

3.1. Adsorption kinetics ……S9

3.2. Desorption process ……....S10

3.3. Effect of the temperature on the adsorption process…….….S10

3.4. Effect of the adsorbent quantity……...S11

3.5. Effect of initial metal ion concentrations and isotherm analysis ……..S12

4. Thermodynamic studies of the adsorption process…….……..S15

5. References ……...S17

1. Experimental section

1.1. Reagents and materials

All reagents were of analytical grade. Iron (II) chloride tetrahydrate ($FeCl_2.4H_2O$, 99.0%), was obtained from Shanghai Macklin Biochemical Co., Ltd. (China). Iron (III) chloride hexahydrate ($FeCl_3.6H_2O$, 99.0%) and salts of different cations studied namely $Pb(NO_3)_2$ (99.0%), $CuCl_2$ ($\geq$ 98.0%), and $NiCl_2$($\geq$ 98.0%) were purchased from Sinopharm Chemical Reagent Co., Ltd. (China). Hydrazine hydrate ($N_2H_4.H_2O$), sodium hydroxide (NaOH), hydrochloric acid (HCl, 12 M), nitric acid (16 M) and ethanol were obtained from Shanghai Lingfeng Chemical Reagent Co., Ltd. (China). $CdCl_2$ (99.996%) was purchased from Alfa Aesar (China) Chemical Co., Ltd. All chemicals were used as received without further purification.

Milli-Q system (Millipore, USA, 18.2 MΩ cm) for deionized water was used throughout the experiments. MP 220 Mettler- Toledo pH meter coupled with a pH combination polymer electrode was used in pH measurements.

The crystallinity of the powder Fe_3O_4 was determined by X-ray diffraction (Rigabu D/max VB/PC X-ray diffractometer using nickel-filtered CuKα1 radiation (λ = 1.54056 Å). The surface morphology and particle size of the Fe_3O_4 nanoparticles were characterized by A JEOL, JEM-100 CX II transmission electron microscopy (TEM) with accelerating voltage 200 kV (JOEL 2010, JOEL Ltd, Japan). The content of metal ions was determined using inductively coupled plasma atomic emission spectrophotometer (ICP-AES,Agilent 725ES).The specific surface area was analyzed by Brunauer-Emmett-Teller (BET) adsorption isotherms at 77 K performed on a volumetric adsorption analyzer ASAP 3020.

1.2. Synthesis procedure of Fe_3O_4 nanoparticles

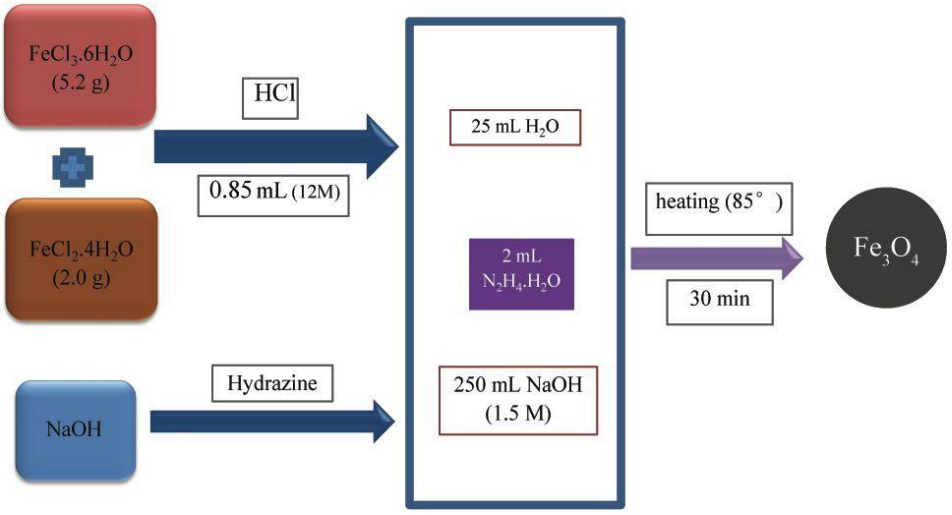

Figure S1: Chemical synthesis route of Fe_3O_4 nanoparticles

1.3. Metal ions removal procedure

In order to remove effectively the different metal ions (Pb^{2+}, Cd^{2+}, Cu^{2+}, Ni^{2+}) from water, certain significant parameters including pH of the analyte solution, adsorbent mass, contact time, temperature, initial metal ion concentrations and desorption processes were investigated. A 1 g L^{-1} stock solution containing each metal ion was prepared separately using deionized water and required dilutions were made to obtain the appropriate concentration in order to obtain the artificial wastewater solutions.

The adsorption equilibrium tests were carried out as follows. In a clean plugged conical flask, 50 mg of the prepared powder Fe_3O_4 was added to 50 mL of metal ion solution with initial concentration of 10 mg L^{-1} at ambient conditions. Subsequently, the mixture was vigorously stirred by a shaker with a speed of 220 rpm at 25°C to allow a complete adsorption of the metal ion by the Fe_3O_4 nanoparticles. After shaking, the mixture was withdrawn from the shaker at regular time intervals of 10 min. And then, a permanent hand-held magnet was used to separate the liquid-phase followed by measuring the residual content of the metal ion using inductively coupled plasma atomic emission spectrophotometer (ICP-AES). To carry out the influence of

the solution pH, the pH values ranging from 2 to 12 of the solution were adjusted by addition of 1 and 0.1 M nitric acid (HNO_3) or 1 and 0.1 M sodium hydroxide solution (NaOH). To further understand the impact of the ultra-fine Fe_3O_4 nanoparticles on the adsorption, diverse amounts of Fe_3O_4 in the range 10 - 200 mg were used to extract the metal ions. The influence of the temperature was also studied. To this aim, the uptake tests were carried out at different temperatures including 5, 25, and 45°C. The experiments were performed by altering one parameter whilst the other parameters were kept constant. Besides, to ensure the reproducibility and reliability of the collected data, all batch tests were evaluated in duplicates and the average value has recorded in the graphs. The effect of contact time revealed the equilibrium time. So, the adsorption equilibrium isotherm was also carried out using different initial metal ion concentrations in the range 10-150 mg L^{-1} at room temperature. Once the equilibrium was achieved, the concentration of the metal ion was measured. Thus, the adsorption capacity[1] of the as-prepared Fe_3O_4 and the percent removal[2] have calculated by the following equations:

$$q_e = \frac{(C_0 - C_e)}{m} V \quad (1)$$

$$\%\text{Removal} = 100\frac{C_0 - C_f}{C_0} \quad (2)$$

where q_e represents the equilibrium adsorption (mg g^{-1}), C_0 and C_e are the initial and equilibrium metal ion concentration respectively (mg L^{-1}), C_f (mg L^{-1}) is the concentration of metal ion after adsorption, m the amount of the as-prepared Fe_3O_4 (g), and V is the volume of the solution containing the metal ion (L).

The desorption study was performed to test the reusability of the nanoadsorbent. For this purpose, 50 mg of Fe_3O_4 nanoadsorbents were used to adsorb each ion tested in 50 mL of 10 mg L^{-1} of ion. Thus, after reaching the adsorption equilibrium, the nanoadsorbents were removed and dispersed in 10 mL of diluted nitric acid (0.01 M) for 20 min and shaken for 10 min. Afterwards, the nanoadsorbents were removed using a permanent hand-hold magnet, washed with deionized water several times, and dried for adsorption in succeeding cycles.

1.4. Point of zero charge measurement

The point of zero charge (PZC) is known as the pH value when the net total charge is zero on the surface of a system. Thus, to understand the adsorption process, the PZC remains a fundamental parameter for the adsorbent. Indeed, it allows describing the adsorption of charged species and the effect of the medium's pH on the adsorption. For this aim, the zeta potential of Fe_3O_4 nanoparticles was carried out using Zetazier microelectrophoresis appliance at constant temperature 25°C. This apparatus measures directly the electrophoretic mobility of Fe_3O_4 NPs in dilute dispersions and converts it into zeta potential. For this analysis, 200 µL of the Fe_3O_4 NPs suspension were added to 50 mL deionized water and the pH values in the range 2 - 11 of the suspension was automatically adjusted by addition of 1 and 0.1 M nitric acid (HNO_3) or 1 and 0.1 M sodium hydroxide solution (NaOH).

2. Characterization of the magnetite nanoparticles

2.1. Brunauer-Emmett-Teller study after adsorption

The pore size distribution curve of the metal ions tested after adsorption is shown in Figure S2 in which various peaks are observed. It was found that after adsorption the pore became smaller due to the drying pretreatment and the adsorbed metal ions. And the average diameters are between 2.5 and 3.6 nm. Importantly, the surface area of Fe_3O_4 NPs loaded with Pb^{2+}, Cd^{2+}, Cu^{2+}, and Ni^{2+} ions were found to be 109.45, 109.83, 117.43, and 108.66 $m^2\ g^{-1}$, respectively. The increase in the surface area after adsorption can be explained by the adsorbed metal ions and the aggregation or overlapping of adsorption sites.

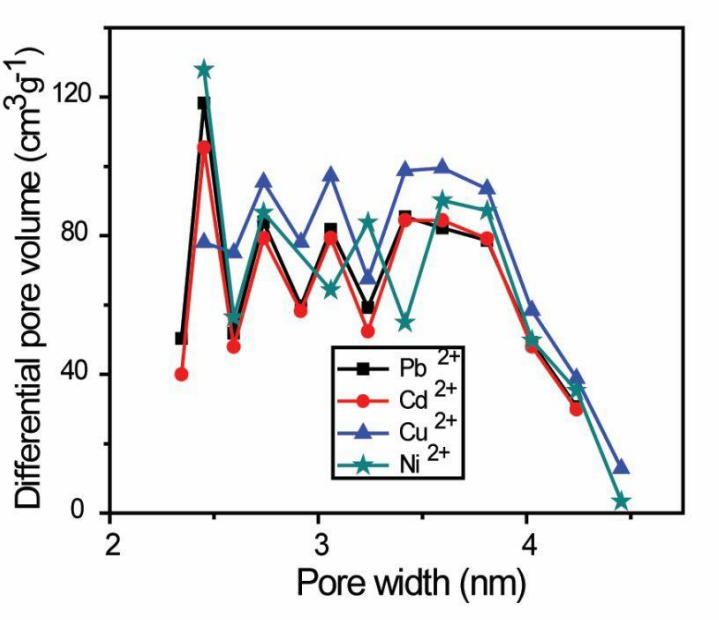

Figure S2 Pore-size distribution curves of Fe_3O_4 NPs after adsorption of metal ions.

2.2. Scanning electron microscope/energy-dispersive X-ray analysis

To further characterize the adsorption, Figure S3A shows the SEM images of the prepared UFMNPs that indicates the surface topography before metal ions adsorption. It can be observed the aggregation of various ultra-fine particles exhibiting spherical shape and confirming the results predicted in the XRD pattern. Details about the morphology of UFMNPs were evaluated after adsorption in the SEM studies. The Figures S3b – S3e indicate the SEM images of UFMNPs loaded with Pb^{2+}, Cd^{2+}, Cu^{2+}, and Ni^{2+} ions, respectively after adsorption. It was clear be seen a demarcation in the surface morphology compared to the intact UFMNPs due to the metal ions exchange reactions and their adsorption via precipitation. In order to prove the adsorption of the metal ions studied, EDX spectra were recorded and can be observed in Figures S3(f-j). As can be seen, the spectrum of unloaded UFMNPs (Figure S3f) shows none peak of the tested metal ions, whereas the EDX spectra S3g-S3j of the ions loaded UFMNPs show the characteristic peaks of Pb^{2+}, Cd^{2+}, Cu^{2+}, and Ni^{2+} ions indicating they have been successfully adsorbed on the UFMNPs surface.

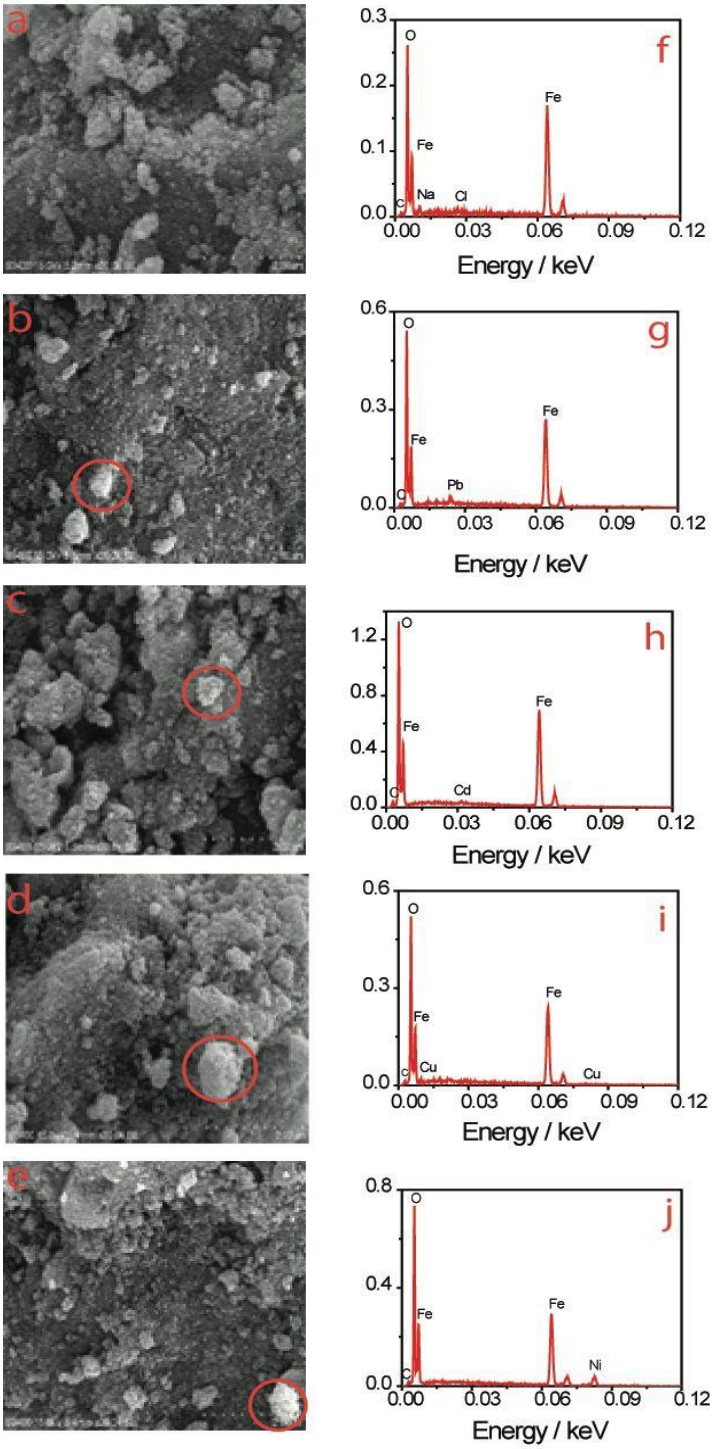

Figure S3 SEM images of the Fe_3O_4 NPs a) before metal ion adsorption and after b) Pb^{2+}, c) Cd^{2+}, d) Cu^{2+}, and e) Ni^{2+} ions adsorption. EDX spectra of the Fe_3O_4 NPs f) before metal ion adsorption and after g) Pb^{2+}, h) Cd^{2+}, i) Cu^{2+}, and j) Ni^{2+} ions adsorption. (Metal ions concentrations 10 mg L^{-1}). Scale bars in a-e: S3400 15.0 kV 5.2 mm x 20.0 k SE (2.00 µm). Red circles in a-e show adsorbed metal ions.

3. Tests of the metal ions adsorption

3.1. Adsorption kinetics

The pseudo-first-order kinetic model of the Lagergren [3] is one of the most widely used for the adsorption of a solute from liquid solutions and can be expressed in linear form by Equation 3. While the chemisorption pseudo-second-order [4] is a surface-interaction kinetic model and can be expressed in linear form by equation 4.

$$\ln (q_t - q_e) = lnq_e - \Gamma_1 t \quad (3)$$

$$\frac{t}{q} = \frac{1}{\Gamma_2 q_e^2} + \left(\frac{1}{q_e}\right) t \quad (4)$$

where q_t and q_e (mg/g) are the quantity of metal ions adsorbed onto the nanoadsorbent at any time and equilibrium time, respectively. Γ_1 (min^{-1}) and Γ_2 (g $mg^{-1}min^{-1}$) represent the rate constants of the pseudo-first-order and pseudo-second-order kinetics, respectively. The values Γ_1 and q_e (Equation 3) are obtained from the slope and the intercept of the plotting $\ln (q_t - q_e)$ versus t, respectively. The values Γ_2 and q_e (Equation 4) are evaluated from the slope and intercept of the straight line of the plotting t/q against t, respectively.

Table S1: Experimental findings on the adsorption of metal ions tested from mixed and single solutions (river water).

Metal ion (50 mg L^{-1})	K_d (mL g^{-1})	Removal efficiency (%)	q_e (mg g^{-1})	K_d (mL g^{-1})	Removal efficiency (%)	q_e (mg g^{-1})
	Single			**Mixed**		
Pb^{2+}	20333	98	24	2978	86	21
Cd^{2+}	3216	87	22	2039	80	20

Cu^{2+}	4263	90	22	2705	84	21
Ni^{2+}	1461	75	19	592	54	14

3.2. Desorption process

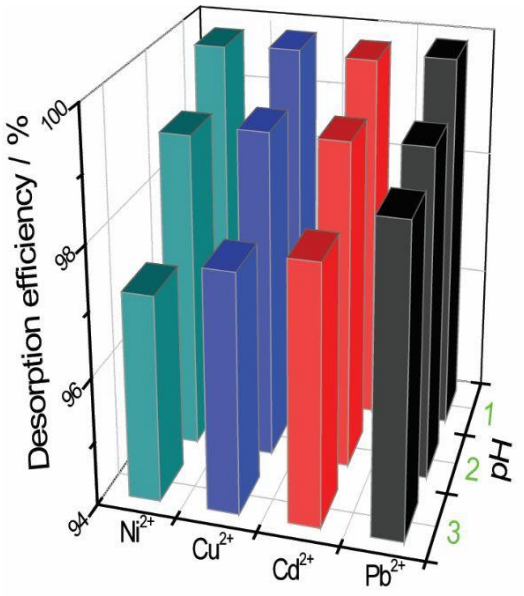

Figure S4 Effect of different pHs of diluted nitric acid on Cu^{2+}, Cd^{2+}, Ni^{2+}, Pb^{2+} ions desorption efficiency

Table S2: Parameters of kinetic models for Cu^{2+}, Cd^{2+}, Ni^{2+}, Pb^{2+} ions removal onto Fe_3O_4 NPs and their correlation coefficient (R^2).

		Single adsorption				Competitive adsorption			
Kinetic models	**Parameters**	Pb^{2+}	Cd^{2+}	Cu^{2+}	Ni^{2+}	Pb^{2+}	Cd^{2+}	Cu^{2+}	Ni^{2+}
Pseudo-first-order	q_e (cal.)(mg g^{-1})	4.59	3.65	11.72	10.91	0.95	19.83	16.25	33.03
	Γ_2 (min^{-1})	0.023	0.038	0.048	0.034	0.036	0.041	0.035	0.042
	R^2	0.9092	0.7555	0.8787	0.9909	0.7044	0.6970	0.8664	0.4865
Pseudo-second-order	q_e (cal.)(mg g^{-1})	25.06	21.88	22.99	20.53	21.55	20.62	20.27	15.43
	Γ_2 (min^{-1})	0.045	0.025	0.011	0.004	0.010	0.005	0.008	0.003
	R^2	0.9997	0.9999	0.9997	0.9995	0.9999	0.9981	0.9981	0.9877
Experimental	q_e (exp.)(mg g^{-1})	24.40	21.64	22.38	18.63	21.41	20.08	21.10	13.55

3.3. Effect of the temperature on the adsorption process

The effect of temperature upon the adsorption was carried out at three different temperatures namely 5, 25, and 45°C and shown in Figure S5. The experimental findings indicated that the removal efficiency increases with the increase of the temperature from 5°C to 45°C. This observation is due to the change in the size of the pore causing a swelling effect within the internal structure of the Fe_3O_4 nanoadsorbents which facilitates the uptake of metal ions.[5] Additionally, the increase in the temperature provoked an increase in the mobility of metal ions number of active sites on Fe_3O_4 nanoadsorbents for the adsorption with increased temperature. Consequently, the temperature influences positively the adsorption of heavy metal ions and the adsorption of the investigated metal ions is endothermic. It is well-known that the adsorption process is mainly impacted by the temperature in term of the diffusion rate of adsorbate substances and the internal pores of the adsorbent materials. Therefore, the diffusion rate increases by raising the temperature generating a decrease in the viscosity of the solution. The increase in the temperature increases thus the efficiency removal of UFMNPs for the studies metal ions.

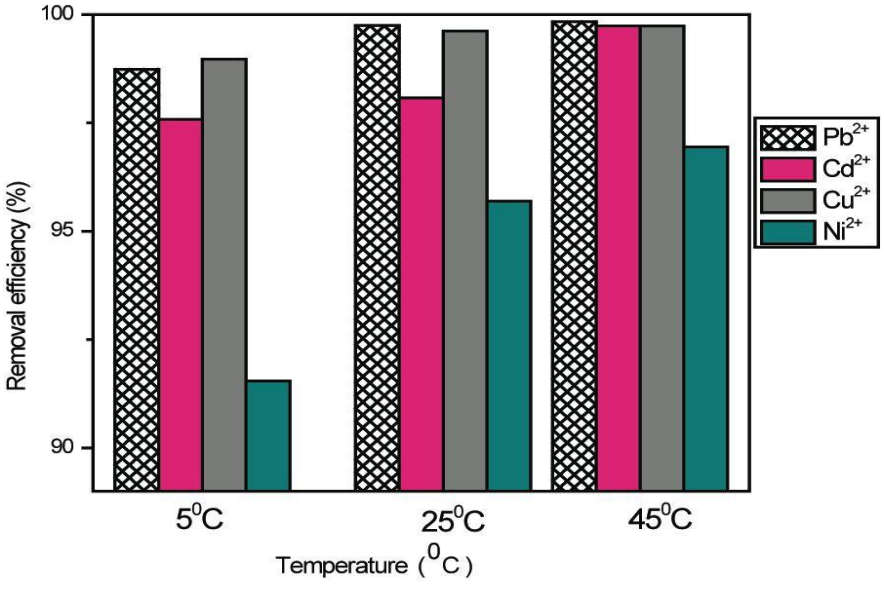

Figure S5: Effect of the temperature on adsorption of Cu^{2+}, Cd^{2+}, Ni^{2+}, Pb^{2+} ions at fixed pH 5.5.

3.4. Effect of the adsorbent quantity

One of the most important parameters in adsorption process that determine the adsorbent capacity for a known initial metal ion concentration is adsorbent amount. Figure S6 depicts the effect of the adsorbent amount on the adsorption of heavy metal ions. As can be seen, all investigated metal ions exhibit similar behavior. Indeed, when the adsorbent amount increased the uptake efficiency also augments up to reach a maximum and then becomes almost constant. The increase in adsorption of metal ions can result from the increase of the number of active sites and the increase in nanoadsorbents surface area with the increase Fe_3O_4 nanoadsorbents amount facilitating thus a rapid penetration of metal ions to the sites.[5] The observed "plateau" in the removal efficiency of UFMNPs toward the different tested metal ions reveals that no further increase in UFMNPs doses impacted on the uptake of these metal ions.

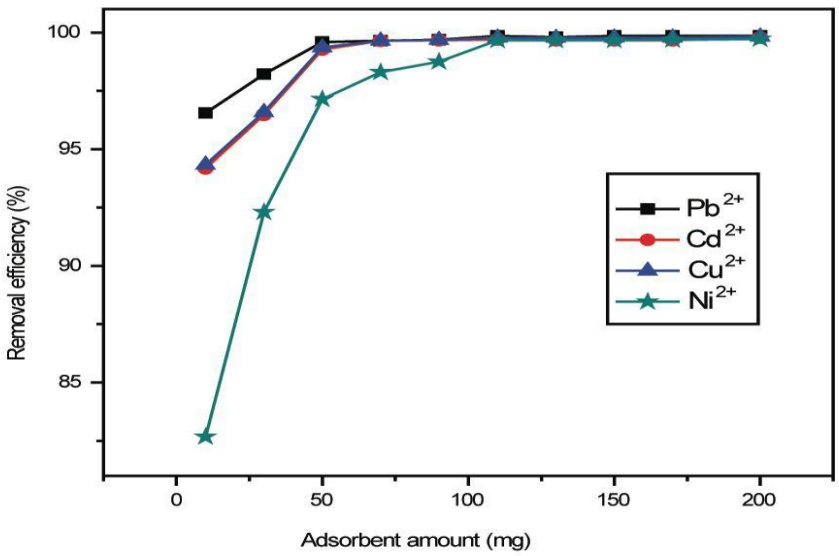

Figure S6 Effect of adsorbent doses on adsorption of Cu^{2+}, Cd^{2+}, Ni^{2+}, Pb^{2+} ions (initial concentration 10 mg L^{-1}, 50 mL solution, initial pH of solution 5.5, temperature 25°C).

3.5. Effect of initial metal ion concentrations and isotherm analysis

To determine the nature of the interaction between all tested metal ions and the Fe_3O_4 nanoadsorbents and find the maximum capacity of these nanoadsorbents, the adsorption data were examined using adsorption isothermal models such Langmuir, Freundlich, Dubinin-Radushkevich, and Temkin isotherm models.

In Langmuir isotherm model [6], it is assumed uniform energies of the adsorption onto a homogeneous surface and the adsorption should be limited to the formation of a monolayer. It linear form is represented as follows:

$$\frac{C_e}{q_e} = \frac{1}{K_L q_M} + \left(\frac{1}{q_M}\right) C_e \quad (5)$$

where q_e(mg g^{-1}) is the equilibrium amount of metal ion adsorption, C_e(mg L^{-1}) represents the equilibrium concentration of metal ion in solution, q_M(mg g^{-1}) refers to the maximum adsorption capacity, K_L(L mg^{-1}) is the Langmuir constant. K_L and q_M values are determined from the linear plot $\frac{C_e}{q_e}$ versus C_e.

The main characteristic of Langmuir isotherm can be used to predict the nature of the adsorption between the metal ion and the nanoadsorbent using the separator factor R_L defined by [7]:

$$R_L = \frac{1}{1 + K_L C_0} \quad (6)$$

where C_o(mg L^{-1}) indicates the highest initial concentration of the metal ion. The values of R_L are $0 < R_L < 1$, $R_L > 1$, $R_L = 0$, and $R_L = 1$ and assign to favorable, unfavorable, irreversible, and linear adsorption, respectively.

The Freundlich isotherm model [8] assumes that the adsorption process onto heterogeneous surface with various adsorption energies. Its linearized form is given by the following equation:

$$\ln q_e = \ln K_{Fr} + \frac{\ln C_e}{n} \quad (7)$$

where K_{Fr} refers to Freundlich constant, n is a dimensionless factor related to the intensity of adsorption. K_{Fr} and n are obtained from the linear plot $\ln q_e$ against $\ln C_e$. The Dubinin-Radushkevich (D-R) isotherm model [9] was also used to analyze the experimental data to know if the adsorption of the metal ions studied is chemisorption or physisorption. Thus, the linearized form of the model is expressed as follows:

$$\ln q_e = \ln Q_M - B_{DR}[RT\ln(1 + 1/C_e)]^2 \quad (8)$$

where Q_M(mg g^{-1}) refers to the maximum adsorption capacity of metal ion onto Fe_3O_4 nanoadsorbent, B_{DR}(mol^2 J^{-2}) is the activity coefficient related to mean adsorption energy, R(J K^{-1} mol^{-1}) is the gas constant, and T(K) is the absolute temperature. Q_M and B_{DR}can be obtained from the linear plot $\ln q_e$versus $[RT\ln(1 + 1/C_e)]^2$. The mean adsorption energy ε(kJ mol^{-1}) is calculated using Equation (9):

$$\varepsilon = 1/\sqrt{2B_{DR}} \quad (9)$$

The Temkin isotherm model [10] was chosen to examine the interaction nanoadsorbent-metal ions adsorbed. Its linear form is expressed as follows:[10]

$$q_e = \frac{RT}{\delta_T}\ln K_T + \frac{RT}{\delta_T}\ln C_e \quad (10)$$

where K_T(L g^{-1}) and δ_T(J mol^{-1}) represent the Temkin isotherm constant and the constant indicated to the heat of adsorption, respectively. R(8.314 J K^{-1} mol^{-1}) is the universal gas constant. The values of K_T and δ_T can be determined from the Temkin plot of q_e against $\ln C_e$.

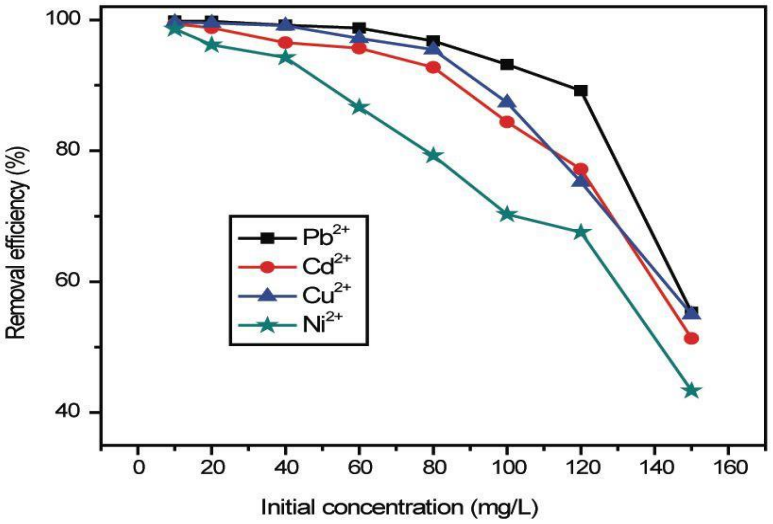

Figure S7: Effect of initial concentration of Cu^{2+}, Cd^{2+}, Ni^{2+}, Pb^{2+} ions on the removal efficiency (initial concentration 10 mg/L, 50 mL solution, initial pH of solution 5.5, temperature 25°C).

Table S3: Isotherm parameters of four different adsorption isotherm models for Pb^{2+}, Cd^{2+}, Cu^{2+} and Ni^{2+} ions.

Isotherm parameters		**Pb^{2+}**	**Cd^{2+}**	**Cu^{2+}**	**Ni^{2+}**
Langmuir isotherm	q_M(mg g^{-1})	85	79	83	66
	K_L(L mg^{-1})	9.08	8.30	8.92	6.95
	R^2	0.9997	0.9966	0.9981	0.9963
Freundlich isotherm	K_{Fr}	48	32	23	39
	n	3.43	3.13	3.07	3.06
	R^2	0.8820	0.8806	0.8504	0.9093
Dubinin-Radushkevich isotherm	Q_M(mg g^{-1})	81	67	75	55
	B_{DR}	$2.2x10^{-3}$	$4.4x10^{-3}$	$3.2x10^{-3}$	$6.8x10^{-3}$
	ε(kJ mol^{-1})	15	11	13	9
	R^2	0.9015	0.8037	0.9299	0.7081
Temkin isotherm	δ_T	227	217	220	200
	K_T	104	71	90	31
	R^2	0.8655	0.8955	0.9204	0.8991

4. Thermodynamic studies of the adsorption process

The thermodynamic study was carried out in term of the calculation of Gibbs parameters such as energy change (ΔG^0), enthalpy change (ΔH^0), and entropy change (ΔS^0). The relationship that typifies these parameters is expressed by Equation 11:[11]

$$\ln k_D = \frac{\Delta S^0}{R} - \frac{\Delta H^0}{RT} = -\frac{\Delta G^\circ}{RT} \quad (11)$$

where ΔG^0, ΔH^0, and ΔS^0 are Gibbs energy parameters in J mol^{-1}, T(K) is the constant temperature for the adsorption, R(J K^{-1} mol^{-1}) represents the universal gas constant, and $k_D = \frac{q_e}{C_e}$ is the adsorption affinity where q_e and C_e are the same already mentioned. The values of ΔH^0 and ΔS^0 are calculated from plotting $\ln k_D$ versus 1/T (Figure S8). Table S4 shows the evaluated values of Gibbs energy parameters. From this Table, for all the tested metal ions ΔG^0 are negative and decrease when the temperature increased indicating that the adsorption process was spontaneous and quite favorable at higher temperature. For ΔH^0 and ΔS^0, their obtained values are positive. The positive value of ΔH^0 suggests that the adsorption process is endothermic and controlled by chemisorption.[12] Likewise, the positive value of ΔS^0 indicates there is increase in randomness at the interface of Fe_3O_4 NPs during the adsorption.[13] Furthermore, this positive value of ΔS^0 confirms the adsorption process is spontaneous owing to the rise of entropy as the system shifts to a state that is more uniform and stable.[14]

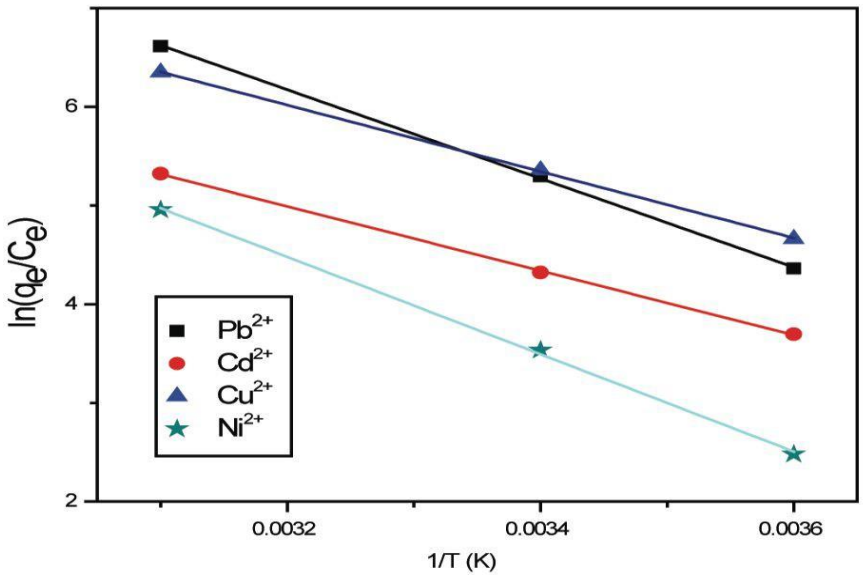

Figure S8: Thermodynamic studies for the adsorption of Pb^{2+}, Cd^{2+}, Cu^{2+}, and Ni^{2+} onto the ultra-fine Fe_3O_4 NPs.

Table S4: Thermodynamic parameters of Pb^{2+}, Cd^{2+}, Cu^{2+}, and Ni^{2+} onto UFMNPs at three different temperatures.

Temperature (K)	Thermodynamic parameters											
	Pb^{2+}			**Cd^{2+}**			**Cu^{2+}**			**Ni^{2+}**		
(kJ mol^{-1})	ΔG^0	ΔH^0	ΔS^0	ΔG^0	ΔH^0	ΔS^0	ΔG^0	ΔH^0	ΔS^0	ΔG^0	ΔH^0	ΔS^0
278	-10.14	37.42	0.17	-8.54	27.12	0.13	-10.82	28	0.14	-5.83	41.02	0.17
298	-13.56			-11.11			-13.61			-9.20		
318	-16.98			-13.67			-16.41			-12.57		

5. References

(1) Altun, T.; Pehlivan, E. Removal of Cr(VI) from aqueous solutions by modified walnut shells. *Food Chem.* **2012**, *132*, 693–700.

(2) Karami, H. Heavy metal removal from water by magnetite nanorods. *Chem. Eng. J.* **2013**, *219*, 209–216.

(3) Laviron, E. General expression of the linear potential sweep voltammogram in the case of diffusionless electrochemical systems. *J. Electroanal. Chem.* **1979**, *101*, 19–28.

(4) Abdel Salam, M.; Al-Zhrani, G.; Kosa, S. A. Removal of heavy metal ions from aqueous solution by multi-walled carbon nanotubes modified with 8-hydroxyquinoline: Kinetic study. *J. Ind. Eng. Chem.* **2014**, *20*, 572–580.

(5) Ozturk, D.; Sahan, T. Design and Optimization of Cu (II) Adsorption Conditions from Aqueous Solutions by Low-Cost Adsorbent Pumice with Response Surface Methodology. *Pol. J. Environ. Stud.* **2015**, *24*, 1749–1756.

(6) Langmuir, I. The adsorption of gases on plane surfaces of glass, mica and platinum. *J. Am. Chem. Soc.* **1918**, *40*, 1361–1403.

(7) Elhafez, S. E. A.; Hamad, H. A.; Zaatout, A. A.; Malash, G. F. Management of agricultural waste for removal of heavy metals from aqueous solution: adsorption behaviors, adsorption mechanisms, environmental protection, and techno-economic analysis. *Environ. Sci. Pollut. Res.* **2016**, *24*, 1397–1415.

(8) Zhang, M.; Gao, B.; Varnoosfaderani, S.; Hebard, A.; Yao, Y.; Inyang, M. Preparation and characterization of a novel magnetic biochar for arsenic removal. *Bioresour. Technol.* **2013**, *130*, 457–462.

(9) Igwe, J. C.; Abia, A. A. Equilibrium sorption isotherm studies of Cd(II), Pb(II) and Zn(II) ions detoxification from waste water using unmodified and EDTA-modified maize husk. *Electron. J. Biotechnol.* **2007**, *10*, 536–548.

(10) Torabian, A.; Panahi, H.; Nabi Bid Hendi, G.; Mehrdadi, N. Synthesis, modification and graft polymerization of magnetic nano particles for PAH removal in contaminated water. *J. Environ. Heal. Sci. Eng.* **2014**, *12*, 105–124.

(11) Fan, H. T.; Wu, J. B.; Fan, X. L.; Zhang, D. S.; Su, Z. J.; Yan, F.; Sun, T. Removal of cadmium(II) and lead(II) from aqueous solution using sulfur-functionalized silica prepared by hydrothermal-assisted grafting method. *Chem. Eng. J.* **2012**, *198–199*, 355–363.

(12) Deng, L.; Su, Y.; Su, H.; Wang, X.; Zhu, X. Sorption and desorption of lead (II) from wastewater by green algae Cladophora fascicularis. *J. Hazard. Mater.* **2007**, *143*, 220–225.

(13) Chen, H.; Dai, G.; Zhao, J.; Zhong, A.; Wu, J.; Yan, H. Removal of copper(II) ions by a biosorbent-Cinnamomum camphora leaves powder. *J. Hazard. Mater.* **2010**, *177* (1–3), 228–236.

(14) Nagpal, U. M. K.; Bankar, A. V.; Pawar, N. J.; Kapadnis, B. P.; Zinjarde, S. S. Equilibrium and kinetic studies on biosorption of heavy metals by leaf powder of paper mulberry (Broussonetia papyrifera).*Water. Air. Soil Pollut.* **2011**, *215* (1–4), 177–188.